Progress in Nuclear Energy 123 (2020) 103273

Contents lists available at ScienceDirect

Progress in Nuclear Energy

journal homepage: http://www.elsevier.com/locate/pnucene

Validation of coupled fission matrix – TRACE methods for thermal-hydraulic and control feedback on the Penn State Breazeale Reactor

Adam Rau, William J. Walters *

Dept. of Nuc. Eng., Penn. State University, 232 Hallowell Bldg., University Park, PA, 16802, USA

ARTICLE INFO

Keywords:
Fission-matrix
TRIGA
TRACE
Multi-physics
Serpent

ABSTRACT

A new method for calculating power shape and critical control rod position is described and validated in view of increasing the fidelity of the Penn State Breazeale Reactor's (PSBR) fuel management code. Currently, the PSBR fuel management code is biased against experimental results and requires the use of empirical correction factors. This is likely due to a combination of assumptions, such as the control rods being fixed in the all-out position and the use of a uniform fuel temperature. The proposed method supplies this data using fission-matrix-based neutronics coupled with TRACE thermal-hydraulics. The fission-matrix-based neutronics relies on Serpent for pre-calculation of fission matrices. Steady-state fuel temperature distributions, power shapes, and control rod positions are calculated through iteration between TRACE and fission matrix calculations. Validation is performed on the coupled TRACE-fission matrix model for powers ranging from 50 kW to 1 MW. For these cases, the RMS average error with experimental data is 12.7 K for instrumented element fuel temperature and $0.07 for reactivity change. Agreement is generally within estimated experimental uncertainty. The effect of various modeling parameters, such as the fuel-cladding gap heat transfer coefficient and the exact radial location of the instrumented element thermocouple, are shown. Finally, the impact of this increased modeling fidelity on the depletion calculation is estimated. In the future, this validation should be repeated on later core loadings of the PSBR where more detailed experimental data is available. Comparison between the current PSBR fuel management code and the proposed model should also be made.

1. Introduction

The Penn State Breazeale Reactor (PSBR) was established in 1955 as an MTR type reactor, and was converted to a TRIGA reactor in 1965. Several fuel management programs have been used over the course of its history (Naughtonet al., 1974; Boyle et al., 1998; Tippayakulet al., 2004; Tippayakul et al., 2008) which have provided successive improvements in modeling fidelity. The current fuel management and core modeling code, TRIGSIMS, couples the Monte Carlo code MCNP (X-5 Monte Carlo Team, 2008) to calculate flux/power distributions and cross-sections with ORIGEN for material depletion. While this method is more robust than older methods, there are still significant biases to current experimental results, which require the use of empirical correction factors for calculations of excess reactivity, D_2O tank reactivity worth, etc. These differences are likely due to a combination of assumptions made in TRIGSIMS, such as control rods being fixed in the all-out position, and the use of a uniform temperature profile fixed at an arbitrary temperature. Relaxing these assumptions may lead to better prediction of experimental results and fluxes, and more economic use of fuel. This is particularly important since the 8.5 and 12 wt% TRIGA fuel used at the PSBR is no longer being fabricated.

A thermal-hydraulic model of the PSBR could be used to supply the fuel management code with an estimate of material temperatures. Several such models have been developed in the past. Gougar (1997) modeled the PSBR using COBRA-IV to determine if installing shutters on the sides of the PSBR core would violate safety limits. He reported difficulty modeling the cross-flow using this tool, and concluded that a more detailed code was needed. Similarly, Uçar (Uçar et al., 2014) performed ANSYS Fluent simulations to ensure that a proposed D_2O tank would not restrict cross-flow to the point that safety limits would be violated. A computational fluid dynamics (CFD) code was chosen due to the complex nature of the geometry. Wargon later confirmed Uçar's

* Corresponding author.
E-mail addresses: awr5209@psu.edu (A. Rau), wjw24@psu.edu (W.J. Walters).

https://doi.org/10.1016/j.pnucene.2020.103273
Received 16 September 2019; Received in revised form 22 December 2019; Accepted 5 February 2020
Available online 28 February 2020
0149-1970/© 2020 Published by Elsevier Ltd.

study through a RELAP5-3D hot channel model of the PSBR core (Wargon, 2015).

More recently, Karriem (Karriem, 2016) added a module to TRIGSIMS for the purpose of adding fuel temperature feedback and a critical control rod position search capability to the code. This methodology coupled the sub-channel analysis code COBRA-TF to MCNP. The method was validated against experiment on critical control rod position and average fuel temperature for three recent PSBR core loadings at full power, and at two lower power levels (700 kW and 800 kW). However, to achieve this agreement, the density of control rod B_4C in the model was artificially adjusted from a literature value of roughly 2.5 g/cc to 1.7 g/cc. Several iterations between MCNP and COBRA-TF are required to converge to a solution. Running MCNP is the most time-consuming step in the depletion calculation, so iterating on these calculations is not desirable.

The current campaign is investigating fission matrix methods because of their potential to reduce the computational cost of such an iteration. A fission matrix is an $n \times n$ matrix which corresponds to the integration of the eigenvalue equation over n spatial cells:

$$F_i = \left(1 / k_{eff}\right) \sum_{j=1}^{n} a_{ij} F_j$$

Or

$$\vec{F} = \left(1 / k_{eff}\right) \boldsymbol{A} \vec{F}$$

where k_{eff} is the multiplication factor of the system, F_i or $\vec{F}$ is the fundamental mode fission source, and a_{ij} are elements of the fission matrix $\boldsymbol{A}$ (Dufek and Gudowski, 2009a), which represent the number of fission neutrons produced in cell i, due to a fission neutron born in cell j. Traditionally, the fission matrix has been used for acceleration (Kitada and Takeda, 2001; Carneyet al., 2014) and convergence verification (Dufek and Gudowski, 2009a; Carneyet al., 2014; Dufek and Gudowski, 2009b; Dufek and Holst, 2016) of Monte Carlo criticality calculations. Recently, there have been efforts to use Monte Carlo programs to calculate a database of fission matrices for a simplified or representative set of problems, and then interpolate and combine these fission matrices to solve a specific case or more complex problem. Fission matrix methods have been applied to spent-fuel pools (Walterset al., 2009), light water reactors (Terlizzi and Kotlyar, 2019) including some whole-core calculations, (Walters et al., 2018; He and Walters, 2019) MSRs (Laureauet al., 2015; Laureauet al., 2017) nuclear thermal propulsion reactors for space travel (Rau and Walters, 2019a, 2019b), and TRIGA reactors. (Topham and Walters, 2018; Topham et al., 2020)

Like the methodology in TRIGSIMS-TH, fission matrix methods also require multiple Monte Carlo simulations. However, fission matrix methods perform this calculation up-front, and then subsequent neutronics calculations can be performed on the order of seconds. This scheme is more advantageous when more iterations are required. For this reason, fission matrix methods have been developed to account for temperature and control reactivity effects in the PSBR (Topham and Walters, 2018). Most recently, Topham et al. (Topham et al., 2020) performed code-to-code validation of fission matrix methods to calculate the fission source distribution and multiplication factor given an arbitrary fuel temperature distribution and control rod position, finding good agreement with Serpent Monte Carlo simulations with the same temperatures and rod positions. These methods were further developed (extended to three dimensions, substituted linear nearest-neighbor interpolation with polynomial interpolation) and again validated against Serpent on a Nuclear Thermal Propulsion type reactor (Rau and Walters, 2019b).

The present work seeks to validate these methods against experimental data so that the methodology can be applied with confidence. In addition to the power-temperature correlation employed previously (Topham et al., 2020), a TRACE model is developed for thermal-hydraulic feedback. There are several benefits to this; TRACE provides distributions of coolant temperature and density in addition to fuel temperature, and may allow for simulation of transients in the future. Additionally, using a model instead of a correlation allows for investigation of sensitivity to uncertain or changing parameters such as the fuel-cladding-gap heat transfer coefficient. Compared to CFD codes, TRACE has a relatively small computation time (because it calculates area-averaged parameters on a relatively coarse mesh), yet includes two-fluid equations for simulation of two-phase flow.

It should be noted that TRACE was developed to analyze light water reactors, so the current problem (natural circulation flow near atmospheric pressure) is outside the range of cases for which TRACE was developed and assessed. Also, TRACE neglects viscous shear stresses between fluid cells, so it is not expected that the present code will model flow in the open pool with high fidelity. However, the state-of-the-art thermal-hydraulic modeling capabilities packaged in TRACE (such as multi-dimensional fluid dynamics, flow-regime-dependent constitutive equations, and comprehensive heat transfer capabilities) combined with its widespread use make it an appealing choice. Considering the relatively small impact of coolant properties on TRIGA validation data noted in previous works (Cammiet al., 2016), this code is expected to have adequate fidelity to model coolant temperature and density effects in the PSBR.

Researchers at other TRIGA reactors have developed and validated coupled neutronic/thermal-hydraulic codes for similar purposes. Researchers at the University of Pavia performed significant work validating their Monte Carlo models of TRIGA reactors (Borio di Tiglioleet al., 2010; Alloniet al., 2014) and have recently coupled the model to computational fluid dynamics simulations in order to characterize the reactor at full-power steady-state (Cammiet al., 2016). Researchers at the Jožef Stefan Institute have performed work analyzing a CFD-Monte-Carlo neutron transport coupling scheme and validating their models against fuel and coolant temperature (Henry et al., 2017). More recently, they have expanded this model to simulate transient behavior, and have reproduced TRIGA behavior for short transients where the mass flow through the core remains constant (Henry et al., 2018).

2. Methods

2.1. PSBR description

The Penn State Breazeale Reactor (PSBR) is a pool-type TRIGA reactor with a movable core. The reactor operates up to 1 MW steady-state power, and also operates in ramp, pulse, and square-wave modes. The core is cooled by natural circulation, although a pump is used above the core to delay transport of nitrogen-16 to the pool surface before it decays. Additionally, a small pump and heat exchanger are present outside the pool to maintain water temperature during long periods of operation. The fuel is a mixture of uranium and zirconium-hydride, which also provides most of the moderation for the reactor due to its high density of hydrogen. The uranium is enriched to slightly below 20 wt% ^{235}U, while the fuel mixture is either 8.5 or 12.0 wt% U, with the balance being $HZr_{1.7}$ or $HZr_{1.65}$, respectively. The fuel composition gives it a strong negative temperature reactivity coefficient due to thermal up-scattering.

The PSBR is operated through the movement of four control rods. Three of the rods have additional fuel below the absorber, known as fuel-followers. Both fuel rods and fuel-followers contain a zirconium rod in the center. The PSBR can also be loaded with instrumented fuel elements, which have three thermocouples embedded in the fuel.

2.2. Serpent model

A Serpent (version 2.1.30) Monte Carlo model is used to obtain a fission matrix database and to verify the fission matrix calculations

(Leppänenet al., 2015). The present work models core loading 4, which operated from January 1967 to April 1968 (Ross, 1969). Core loading 4 is the first major loading pattern modeled by current fuel management codes at the Penn State Breazeale reactor, and measurements of instrumented thermocouple temperature and reactivity loss as functions of reactor power are given in historical reports (Ross, 1969). Core loading 4 is shown in Fig. 1. Fig. 1 also includes labels for the various control rods in the PSBR core, as well as the instrumented fuel element. As in previous works (Topham and Walters, 2018; Topham et al., 2020), the Serpent multiphysics interface is used to simply add distributions of thermal-hydraulic properties into Serpent. ENDF/B VII.1 cross-sections were used for all materials, while ENDF/B VII.0 S(α, β) scattering data was used.

2.3. TRACE model

In order to simulate thermal hydraulic feedback, a TRACE (version 5 patch 3) model of the Penn State Breazeale reactor was developed. The initial TRACE model was adapted from the work of Garfola et al. (Garfolaet al., 2014).

2.3.1. Material properties

TRACE includes built-in material property correlations for many materials relevant to reactor simulation (U.S.NRC, 2017), and also allows users to define their own material property correlations. Properties for aluminum cladding and concrete (used to model heat transfer through the pool wall) were present in the original model obtained from Garfola et al. (Garfolaet al., 2014) and were not modified for the present work. Material properties for $UZrH_{1.7}$ with 8.5 wt% U and $UZrH_{1.65}$ with 12 wt% U were programmed into the model (IAEA, 1992). Built-in correlations for Boron Nitride were used for graphite reflectors and for the boron carbide neutron absorber material, since specific heat of these materials is similar and since the thermophysical properties of the reflectors and absorber is expected to be relatively unimportant. Similarly, built-in material properties for zircaloy were used in lieu of zirconium.

2.3.2. Hydrodynamic cell nodalization

Fluid flow in the PSBR core was modeled using a "vessel" component, which simulates three-dimensional fluid flow. The core region uses 7 radial nodes, 6 azimuthal sectors, and 10 axial levels to model flow in the core. TRACE allows vessels to be nodalized with either a cylindrical or cartesian coordinate scheme; following the previous work (Garfolaet al., 2014) the vessel was nodalized with a cylindrical coordinates. Although a cylindrical coordinate system was used, flow areas and hydraulic diameters are specified independently to reflect the hexagonal mesh shown in Fig. 2a. This hexagonal mesh was also used to map pin powers to fluid cells. Of course, there is not a one-to-one correspondence between hexagonal and cylindrical sectors; radii of the vessel rings were calculated by averaging the radius of gaps between elements on each side of the hexagons shown in Fig. 2a. The resulting radial rings are shown superimposed on the core loading in Fig. 2b. Five axial levels are used to simulate the fuel region, and one axial node is used for the lower grid plate, one for the upper grid plate, one for the graphite below the fuel, one for the graphite above the fuel, and one for the space between the lower grid plate and the bottom of the fuel elements.

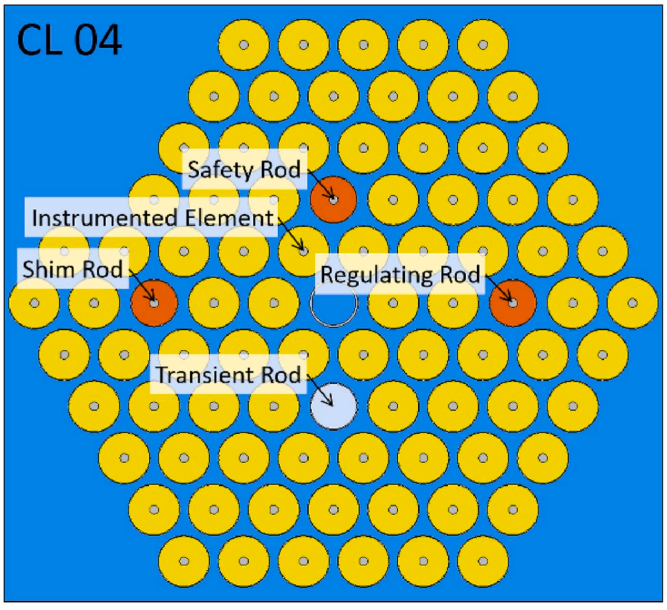

Fig. 1. PSBR Core loading 4. The 8.5 wt% fuel pins are shown in yellow, and fuel-followers/control rods are shown in orange

An additional vessel component was used to simulate flow in the reactor pool. A vessel component is used so three-dimension flow phenomena, such as radial flow into and out of the sides of the core, and intake into the facility heat exchanger, are captured. The pool vessel consists of two radial rings, one azimuthal sector, and 21 axial cells. The pool vessel has one axial level for each of the axial levels in the core, one to simulate the safety plate below the core, two to simulate the offtake and return from the pool heat exchanger, six to simulate flow in the pool. The topmost level is filled with air, and the level below is partially filled with water so that the pool level can be simulated. An atmospheric pressure boundary condition is imposed at the top of the vessel. The component is modeled using a constant mass flow, heat transfer coefficient, and sink temperature presented by Ross (1969). The various components and their connections are pictured in Fig. 3a.

2.3.3. Heat transfer nodalization

In general, at least two heat structures are coupled to each fluid cell in the core vessel, one for fuel elements on the inner edge and one for elements on the outer edge. A schematic arrangement of these heat structures is shown in Fig. 3b. When an instrumented element is present, this is modeled with its own heat structure so that input power peaking factors and output fuel temperatures will not be lumped with nearby fuel elements. Additionally, control rod fuel-followers are modeled with their own heat structures. TRACE does not directly simulate movement of heat structures, so fuel-follower movement is simulated by changing the axial power shape.

Each of the fuel rod heat structures is divided into five axial nodes, in keeping with the fission matrix nodalization scheme and work of previous researchers. Since fuel-follower heat structures are extended, these are divided into ten axial nodes. Radially, the heat structures are divided into 10 intervals, one of which simulates the center zirconium rod, one simulates the gas gap, and one simulates the cladding. The remaining seven intervals simulate heat conduction through the fuel. Heat structures are also created to simulate the conduction through the central thimble, fuel element graphite, control rod graphite and absorber material, the pool wall, and the facility heat exchanger.

2.3.4. Gap heat transfer coefficient

Previous researchers have noted that pulsing of TRIGA fuel leads to an increase of steady-state fuel temperature, which has been attributed to the formation of a gas gap between the fuel and the cladding (Simnad, 1981). This has been observed to change steady-state fuel temperature by more than 25 °C. Formation of the gas gap was studied in the PSBR during core loading 36. Operators installed a fresh instrumented element, and measured the steady-state temperature of the element before and after pulsing. At the conclusion of these experiments, researchers estimated a steady-state temperature drop across the gas gap of 27.6 °C. Since data is only available at the instrumented locations near the center of the core, it is assumed that this gap heat transfer coefficient is uniform along the axial length of the fuel. This temperature

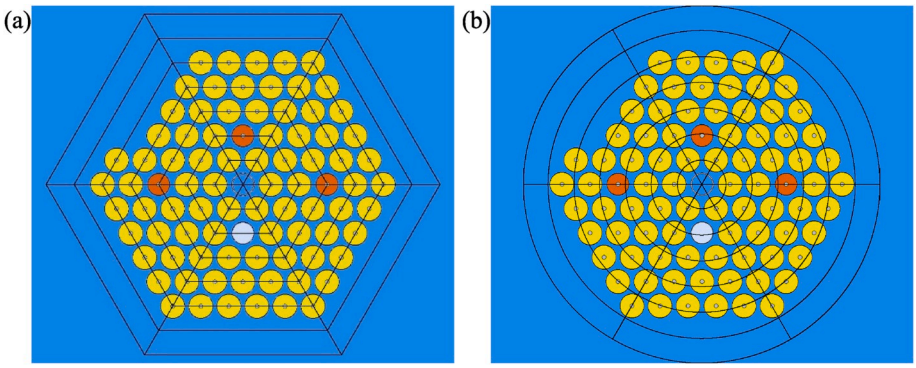

Fig. 2. (a) Hexagonal sectors used to calculate axial, radial, and azimuthal flow areas, and to map pin power to hydraulic cells (b) Radii of cylindrical cells superimposed on core loading pattern.

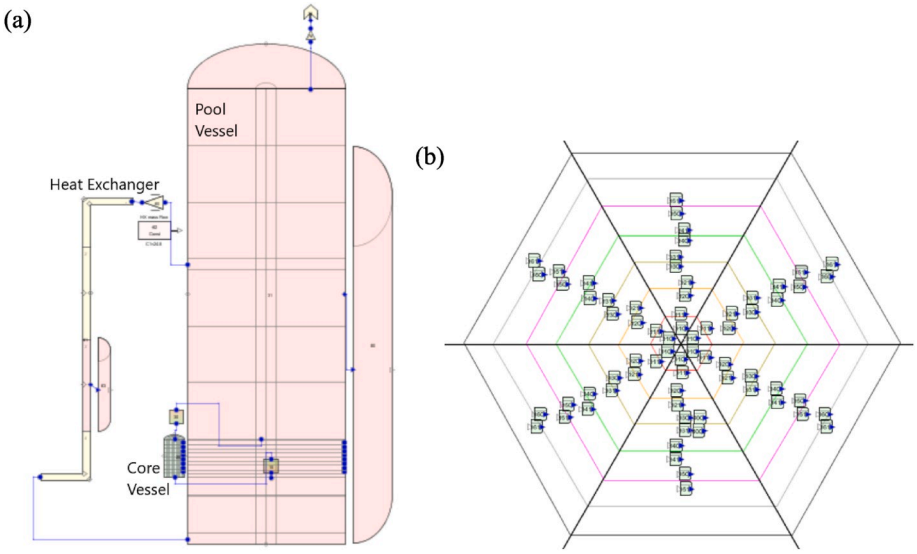

Fig. 3. (a) Fluid components and connections used in TRACE model and (b) Fuel element heat-structures in TRACE model. Each green cylinder represents a heat structure, and cylinders are arranged to show which core fluid cell they are coupled to. Instrumented element heat-structures and fuel-follower heat structures are not shown.

drop can be converted to a heat transfer coefficient:

$$q'' = h_{gap}\Delta T$$

where h_{gap} is the gap heat transfer coefficient, ΔT is the temperature drop across the gap, and q'' is the average heat flux along the surface of the fuel, calculated as

$$q'' = \left(\frac{P}{N_{el}}\right) f_{pin} C_f \Big/ (2\pi R_O L)$$

where P is the nominal core power, N_{el} is the number of fuel elements, f_{pin} is the pin peaking factor for the instrumented element, C_f is a correction factor used to in the PSBR instrumentation to reflect uncertainty in the power calibration, R_O is the outer radius of the fuel and L is the length of the fuel. Using the figures reported in the Safety Analysis Report (Radiation Science and Engineering Center, 2005), the gap heat transfer coefficient is estimated as 1.28×10^4 W/m^{2}K.

This gap heat transfer coefficient is applied to all pins in core loading 4 in the present work. In the initial experiments, steady-state temperature increased after an initial pulse, but successive pulses at the same reactivity did not increase the steady-state temperature further. Pulsing at a higher reactivity or moving the instrumented element to a higher power location would also increase the steady-state temperature. The report (Radiation Science and Engineering Center, 2005) only presents data resulting from \$2.75 pulses in the radial ring adjacent to the central thimble and the next ring outward. Since the maximum pulse performed during core loading 4 was \$2, the heat transfer coefficient used in the present study likely underestimates the actual value in the core center but overestimates at the core periphery.

2.3.5. Wall heat transfer

TRACE uses the flow regime approach to determine heat transfer coefficients between heat structures and fluid cells. Each axial node of each heat structure is assigned a flow regime based on void fraction and saturation temperature in the fluid cell as well as wall temperature. Depending on the regime, TRACE will use different constitutive relations to calculate wall heat transfer coefficients. Single-phase liquid and subcooled nucleate boiling regimes are of primary interest since these occur during regular operation of the PSBR (Haag and Levine, 1973), and both of these are modeled in TRACE. Detailed information on these methods can be found in the "Wall Heat Transfer Models" chapter of the TRACE theory manual (U.S.NRC, 2017).

2.3.6. Radial pin power profile

A fixed radial pin power profile is used in all TRACE simulations. This profile was estimated using a Serpent simulation at room temperature with all control rods fully withdrawn. A cylindrical detector with

30 concentric rings was used to tally the fission source in the instrumented element. The profile, shown as the local power density normalized by the average power density, is plotted in Fig. 4. Power is assumed to be proportional to the fission source, so zero-valued points are non-fuel sections of the pin. The assumption is made that no energy is deposited in the zirconium rod or the cladding since both the power density and the volume of these regions is relatively small, so the total power in these materials should also be relatively small. Nonlocal heating of the coolant is discussed in Section 3.2.

2.4. Şahin fuel temperature correlation

Experimental correlations used by previous researchers are presented for comparison with the TRACE model. Şahin and Ünlü (2012) correlated thermocouple temperature to local power:

$$x = P_{reactor} \cdot \left(P_{local}/P_{max}\right) \cdot 10^{-3}$$

$$T_{TC} = \begin{cases} 294.07 + 1293.13x - 1933.8x^2 + 1391.94x^3 - 35 & P_{reactor} \leq 400kW \\ 749.23x^{0.34} - 10 & P_{reactor} > 400kW \end{cases}$$

where $P_{reactor}$ is the total reactor power, P_{local} is the local power density and P_{max} is the maximum power density. Power is provided in MW and fuel temperature at the thermocouple radius T_{TC} is given in K. This correlation was also used previously (Topham et al., 2020) to model thermal-hydraulic feedback in the PSBR core.

In the current coupled simulations, area-averaged fuel temperature is used to estimate reactivity feedback, and the fuel temperature at a given radius is compared to the instrumented element temperature. Since the correlation presumably provides the thermocouple temperature, some analytical work must be performed to relate this to the area-averaged fuel temperature. This is achieved assuming 1-D radial conduction as in the PSBR Safety Analysis Report (Radiation Science and Engineering Center, 2005).

2.5. Fission matrix methods

Fission matrix methods are used in the present work for their ability to perform fast and accurate neutronics calculations. While the methods themselves are not the focus of the current paper, a brief explanation of the fission matrix methods is included here for completeness.

A cartesian mesh was used for the fission matrix nodalization. A cartesian mesh was selected because it allows simple interfacing with the built-in Serpent FMTX option for calculating fission matrices from criticality calculations. In addition to convenience, calculating fission matrices with the correct fission source distribution is also more accurate. Axially, the fission matrix covers the entire length of the fuel, plus the length occupied by the fuel-followers when the control rods are completely inserted into the core. The same axial cell spacing used by previous codes is used here, so the fission matrix has 10 axial cells. Since the PSBR has a hexagonal core loading, two fission matrix cells were assigned per pin, per axial level. The fission matrix nodalization is pictured in Fig. 5.

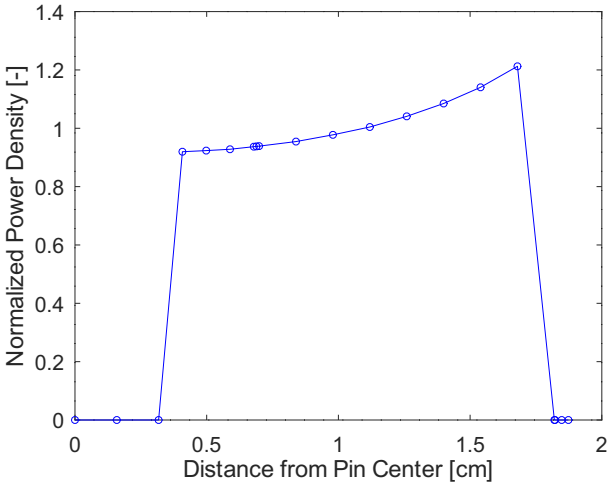

Fig. 4. Radial pin power profile used in TRACE model.

In this work, a database of fission matrices is generated at 5 uniform fuel temperatures (300, 475, 650, 825, and 1000K) and 6 control rod positions for a total of 30 fission matrices. Two additional fission matrices are generated at perturbed coolant temperature and density, resulting in 32 total fission matrices. These database matrices are combined and interpolated in order to estimate a fission matrix for a given temperature distribution and set of rod positions. Further details of the fission matrix methodology will be discussed in a separate paper, but are similar to those discussed in Topham et al. (Topham et al., 2020), the main differences being that methods have been extended to three dimensions, that polynomial interpolation, (rather than piecewise bilinear interpolation), is being used to interpolate between reference fission matrix elements, and that coolant temperature and density effects are modeled.

2.6. TRACE-fission matrix coupling

The present coupling is able to find steady-state, critical control rod positions and distributions of power, fuel temperature, coolant temperature, and coolant density. The steady-state is found through Picard iteration between TRACE and the fission matrix method. Critical rod positions are found by iterating on control rod position until the k_{eff} resulting from the fission matrix calculation matches the desired value within $\pm 0.5\,pcm$. The resulting power shape is then fed into TRACE. TRACE simulations are not run to a true steady-state, but are run for a designated length of time on each iteration. The length of the TRACE simulation was selected by observing the amount of time required for figures of merit to reach steady values; though TRACE has a steady-state capability, the PSBR never achieves a true steady state, but rather a quasi-steady-state where pool water temperature increases slowly.

3. Validation

Validation was performed by comparing the coupled fission matrix-TRACE model with the instrumented element thermocouple temperature and reactivity loss found through experiment. Validation of the underlying Serpent model has been reported in other work (Harris and Walters, 2019).

3.1. Experimental uncertainty and nominal model

Various uncertainties in the experimental data were considered. One such uncertainty arises since the data was not tabulated, but was digitized from plots. However, the same data was presented in multiple plots, so uncertainty was assessed by digitizing both and comparing the results. There is also some uncertainty in the power calibration since the experiments were performed when the core was first brought to power. Operators were aware of this uncertainty at the time, and accounted for it by including a factor of safety when displaying the power on the control console. This factor of safety is used as uncertainty in the power, which is then converted to an uncertainty in the fuel temperature or reactivity loss by fitting a polynomial to the experimental data. Finally, the azimuthal angle of the instrumented fuel element is not known, which affects the location of the thermocouple. Haag and Levine (1973) investigated the effect of azimuthal angle on the fuel temperature; their results are used to predict uncertainty here. The results of these assessments are included in Table 1, and this uncertainty is reflected by error bars on all plotted experimental data.

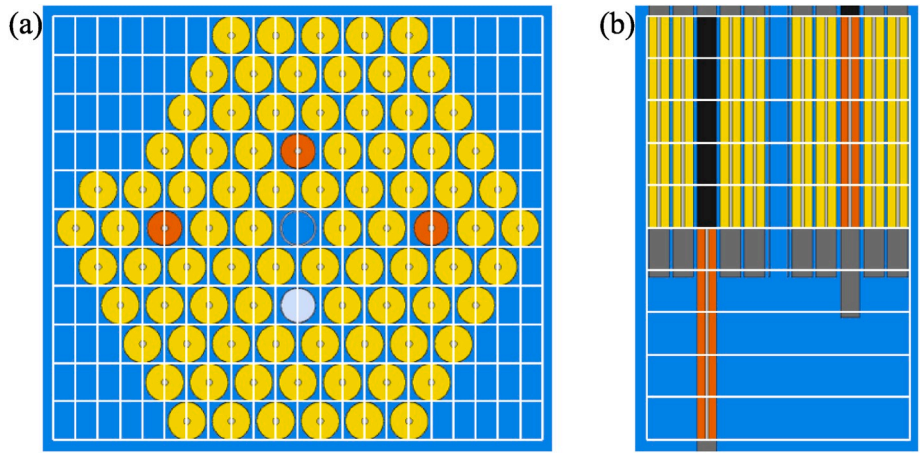

Fig. 5. Lateral (a) and axial (b) fission matrix nodalization.

Fig. 6 compares the results from the coupled fission matrix-TRACE simulations to the experimental data. Over all the cases, the RMS-average temperature error is 12.7 °C and reactivity error is $0.07. The maximum temperature error is 19.4 °C and the maximum reactivity error is $0.14.

3.2. Effect of thermal-hydraulic modeling

While good agreement is observed between the simulation and the experiment data, the metrics examined in the current work are sensitive to several modeling choices. For example, the size of the gap between fuel and cladding and its effect on heat transfer can be difficult to characterize. For this reason, the simulations are repeated using a correlation for the gap heat transfer coefficient developed for the IPR-R1 TRIGA reactor (Mesquita, 2006)

$$h_{gap} = 0.0239q^2 - 1.4372q + 1593.1$$

where h_{gap} is the gap heat transfer coefficient in W/m^{2}K, and q is the reactor power in kW. Although this correlation was developed over a smaller power range (108–265 kW) than that of the PSBR (up to 1 MW), it was investigated here because it was used in previous PSBR modeling efforts (Uçar et al., 2014; Garfolaet al., 2014) and it shows the sensitivity to this coefficient. Results using this correlation are shown in Fig. 7. Unsurprisingly, the correlation developed for the PSBR more closely matches the data.

Due to the large temperature gradient across the radius of a fuel pin, the instrumented element temperature is sensitive to the radial position of the thermocouple, as has been noted by previous researchers (Cammiet al., 2016; Henry et al., 2017). The radial coordinate of the measurement point is not known exactly, and could be affected by tolerances in the installation of the thermocouple or by the physical size of the sensor. The FM-TRACE model estimates the radial coordinate as the center of an equilateral cylinder at the bottom of the thermocouple channel, as shown in Fig. 8. This position is 0.790 cm from the radial center of the fuel element. Previous works on the PSBR have cited 0.69 cm as the radial location of the thermocouple (Boyle et al., 1998; Haag and Levine, 1973). Instrumented element temperatures for both of these radii, as well as the line-averaged temperature along the entire thermocouple channel are shown in Fig. 9a. Additionally, to illustrate the potential sensitivity to the thermocouple location, a sample fuel temperature profile is shown in Fig. 9b.

Additionally, these simulations assume that all fission energy is deposited in the fuel. TRACE's "Direct Moderator Heating" (DMH) option, which deposits a fraction of the heat structure power directly into the surrounding fluid, is used to investigate this sensitivity. Results with 0% and 5% direct moderator heating are shown in Fig. 10. Other studies have found less than 3% energy deposition in the coolant for the VERA LWR benchmark problem (Tuominen et al., 2019). Additionally, since most nonlocal energy deposition is due to neutron slowing down (U.S. NRC, 2017) and a significant amount of neutron moderation occurs in the ZrH material, it is expected that the actual amount of direct moderator heating will be less than an LWR case. Regardless, little impact is seen using even 5% DMH.

Finally, validation using the Şahin fuel temperature correlation in lieu of the TRACE model are presented in Fig. 11. The TRACE model appears to yield a closer prediction of the experimental data; there may be a few reasons for this. The TRACE model is able to account for variations in the coolant temperature, velocity, and heat transfer coefficient, which could change depending on the position of an element within the core and depending on the core loading. Further, the power-temperature correlation was developed using a burned 12 wt% U fuel element, which may have a different thermal conductivity and radial power profile than the fresh 8.5 wt% fuel elements used in core loading 4.

While sensitivity to wall heat transfer coefficient is not investigated, it is worth noting that the nominal TRACE-FM model predicts the onset

Table 1
Uncertainties in fuel temperature and reactivity loss associated with experimental data.

Power [kW]	$\sigma_{digitization}$		σ_{power}		$\sigma_{azimuth}$		σ_{total}	
	T [°C]	ρ[$]	T [°C]	ρ[$]	T [°C]	ρ[$]	T [°C]	ρ[$]
50	1.3	0.004	1.4	0.013	1.2	0	2.2	0.014
100	1.7	0.009	2.7	0.025	1.7	0	3.6	0.027
200	2.8	0.018	4.8	0.046	3.0	0	6.3	0.050
300	3.3	0.023	6.5	0.063	3.7	0	8.2	0.067
500	4.5	0.037	8.3	0.084	5.1	0	10.7	0.092
600	4.9	0.041	8.5	0.088	5.0	0	11.3	0.097
800	5.5	0.048	7.2	0.083	6.4	0	11.1	0.096
1000	6.2	0.055	4.0	0.061	7.2	0	10.3	0.082

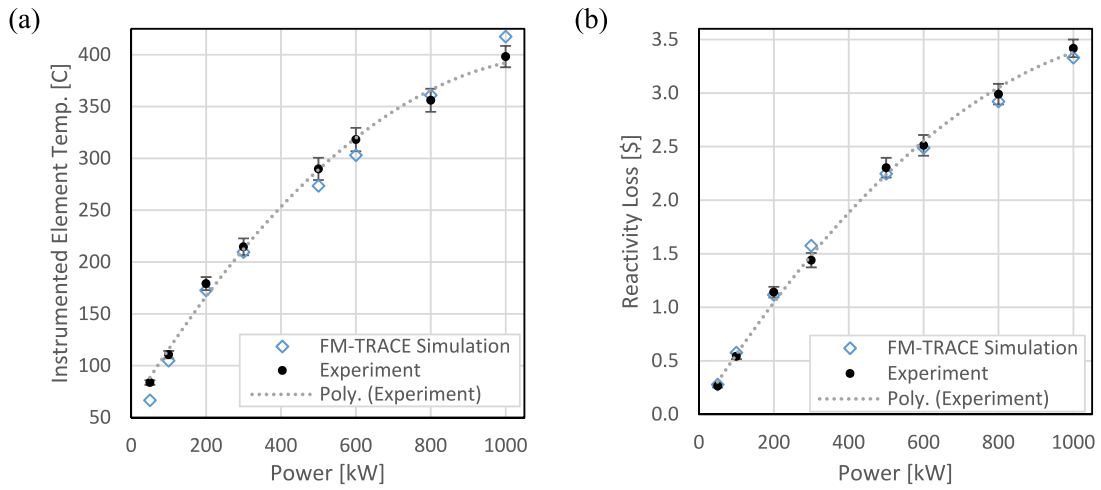

Fig. 6. Comparison of instrumented element temperature (a) and reactivity loss (b) between nominal TRACE-FM simulation and experiment data.

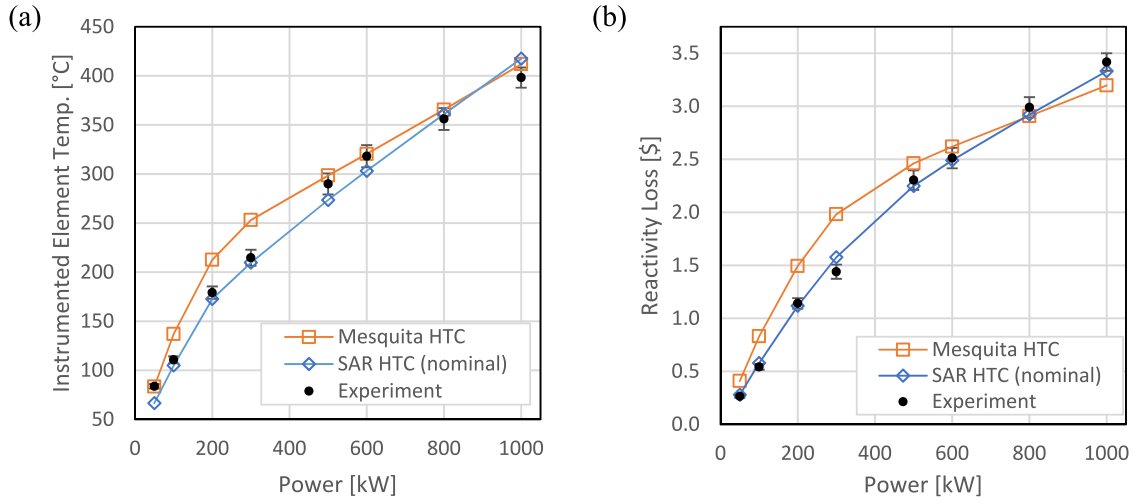

Fig. 7. Comparison of instrumented element temperature (a) and reactivity loss (b) calculated using different fuel-cladding gap heat transfer coefficients. "Mesquita HTC" coefficient comes from a correlation developed for the IPR-R1 TRIGA reactor (Mesquita, 2006) and "SAR HTC" coefficient comes from analysis of pulsing experiments reported in the PSBR SAR (Radiation Science and Engineering Center, 2005).

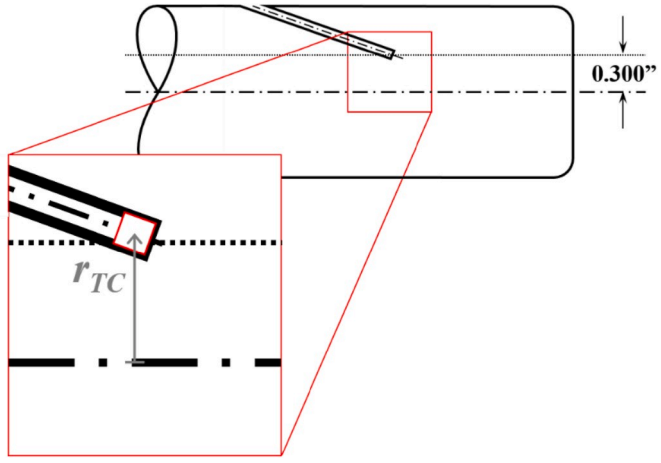

Fig. 8. Modeled radial location of instrumented element thermocouple in TRACE model. The red box represents the equilateral cylinder modeled at the bottom of the thermocouple channel, and the gray arrow shows the radius used to sample the fuel temperature profile in the present work.

of nucleate boiling between 200 and 300 kW. Haag and Levine experimentally observed the onset of nucleate boiling between 150 and 200 kW on a later core loading (Haag and Levine, 1973), so the current model's handling of boiling effects seems reasonable. Uncertainties in this phenomenon could result from surface condition of PSBR fuel pins or the duration of PSBR operation/simulation.

3.3. *Effect of operation strategy*

An additional area of sensitivity is the way that control rods are manipulated to achieve criticality. When the core was first brought to criticality, operators withdrew the safety and transient rods fully while adjusting the power level by manipulating the shim and regulating rods. The nominal simulations in this work mimic this strategy. However, present-day operators of the PSBR generally keep control rods inserted to the same axial level. Choosing one operating strategy or the other can alter the power shape observed in the PSBR, which in turn affects the temperature of the instrumented element. In core loading 4, the instrumented element is adjacent to the safety rod, so the choice to leave this rod fully withdrawn will have a significant impact on the instrumented element temperature. Simulated instrumented element temperatures using both strategies are shown in Fig. 12. Although the

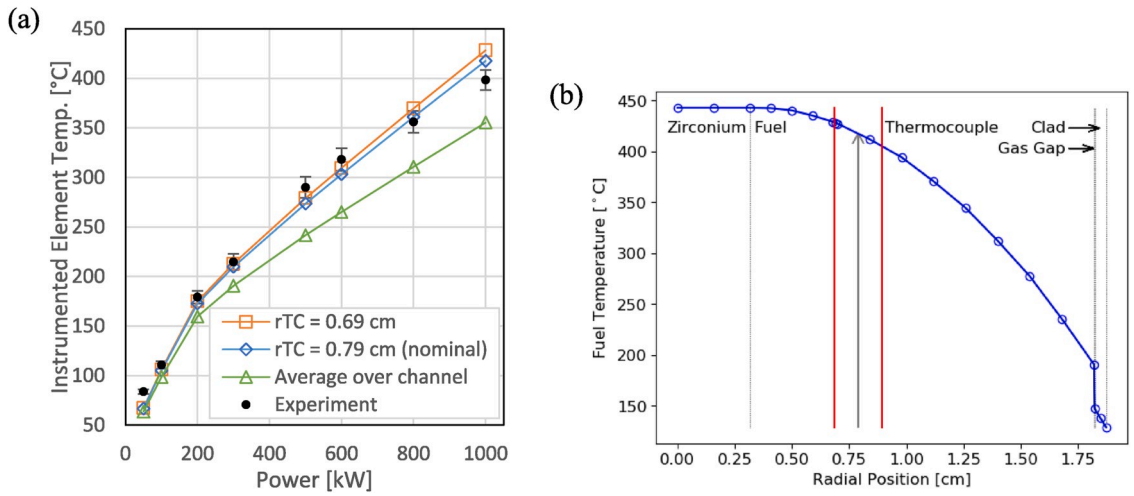

Fig. 9. (a) Comparison of instrumented element temperatures calculated using different radial position of measurement location; (b) Fuel temperature profile for 1000 kW nominal reactor power. Boundaries of the equilateral cylinder used to model the thermocouple are shown in red, and the temperature sampling location is indicated with a gray arrow. Dotted lines indicate material boundaries.

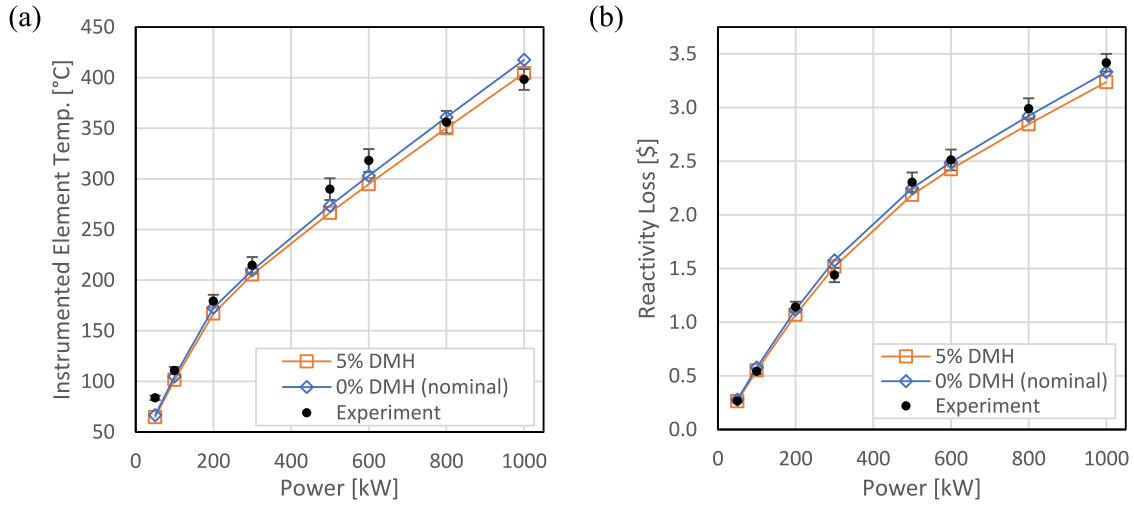

Fig. 10. Comparison of instrumented element temperature (a) and reactivity loss (b) calculated with varying amounts of direct moderator heating (DMH).

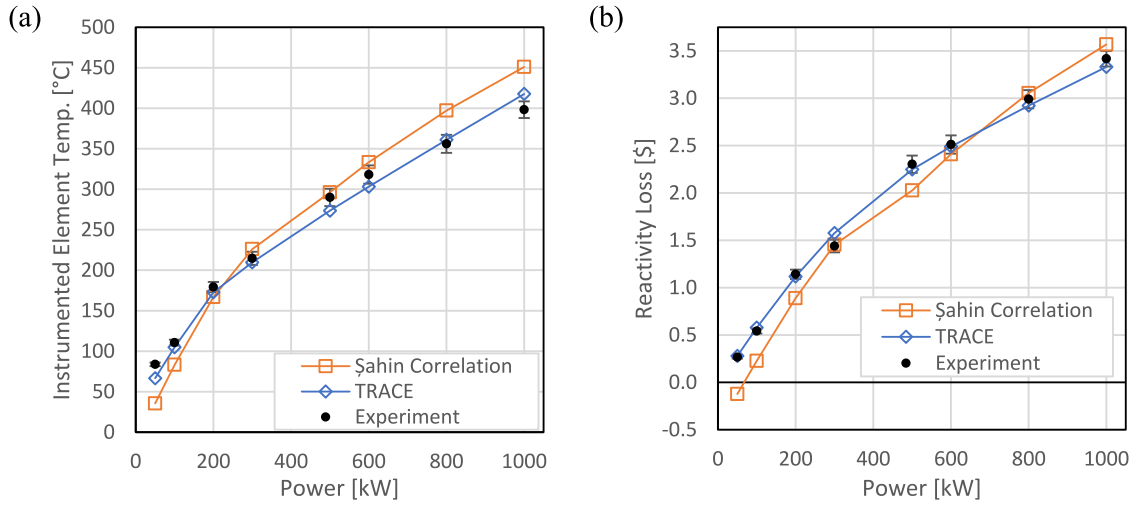

Fig. 11. Comparison of (a) instrumented element temperature and (b) reactivity loss resulting from TRACE program vs. existing correlation.

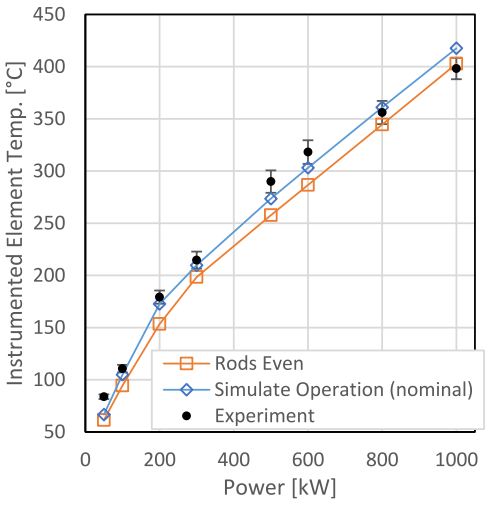

Fig. 12. Comparison of instrumented element temperatures calculated using different rod operation strategies.

difference is small, simulations using the actual rod operation strategy more closely match the data.

3.4. Effect of fission-matrix neutronic modeling

Use of fission matrix methods introduces some error into the calculated power shape and multiplication factor. The magnitude of this error was investigated by performing an additional Serpent calculation using the critical rod positions and steady-state fuel temperature, coolant temperature, and coolant density distributions calculated by the FM-TRACE method. Power shape from this Serpent calculation was used in an additional TRACE calculation to estimate the impact of the power shape error on the instrumented element temperature. An additional Serpent calculation at room temperature and critical rod positions was run in order to estimate the reactivity loss. Because of the additional computational time associated with Serpent calculations, only 100 kW, 500 kW, and 1000 kW were investigated using this technique, and further iterations between TRACE and Serpent were not performed. Validation data calculated using Serpent is shown in Fig. 13. The neutronics modeling appears to have little impact on the instrumented element temperature and reactivity loss calculations.

Finally, although an early loading pattern was selected in order to minimize uncertainty in the fuel burnup, it is not clear whether the experiments were performed at the beginning or the end of the lifetime of core loading 4. To examine this effect, core loading 4 was depleted for using Serpent's depletion routine. Then, instrumented element temperature and reactivity loss were calculated the same way as they were for the Serpent beginning of cycle case. These are also shown in Fig. 13. Overall, Serpent-fission matrix differences are relatively small, but grow slightly (up to $0.12) at full power. The depletion over the cycle has very little effect of both metrics.

4. Modeling impacts

The goal of this model development is to provide higher fidelity fuel-management for the Penn State TRIGA reactor. The present model allows for the relaxation of several modeling assumptions in the current fuel management code; this section explores the impact of relaxing these assumptions. Differences in the power shape are explored in the present section because these errors will propagate to the burnup of specific fuel elements.

The coupled TRACE-Fission matrix approach allows for simple calculation of steady-state fuel temperature profiles and resulting power distributions. The current code uses a static, uniform fuel temperature profile with all rods out when performing depletion analysis. To estimate the impact of calculating a non-uniform temperature, power profiles are calculated for steady-state TRACE-FM fuel temperature distributions and for uniform distributions with the same average temperature. 3D RMS and maximum relative differences between the two power profiles as well as differences in the multiplication factor are shown in Table 2. Differences are calculated as

$$Diff = \left(p_{unif} - p_{dist}\right)/p_{dist} \times 100$$

In addition, relative differences for individual cells at the 1000 kW power level are plotted in Fig. 14. In this figure, the color of each pin represents the relative difference between the two estimations. Positive differences are colored in red, and negative differences are colored in blue. Fig. 14a shows relative differences for fission matrix cells at the axial center of the core (where the largest differences occur), and Fig. 14b shows relative differences at the lowest axial level. It is worth noting that the results in Table 2 and Fig. 14 only show the difference between the TRACE temperature profile and a uniform profile at the same average temperature. In reality, the model that is currently in use will deviate even more because it does not change the power shape as a function of power level.

Although differences in the power shape are small, the uniform temperature case consistently overestimates the multiplication factor. The additional reactivity needs to be compensated by control rod

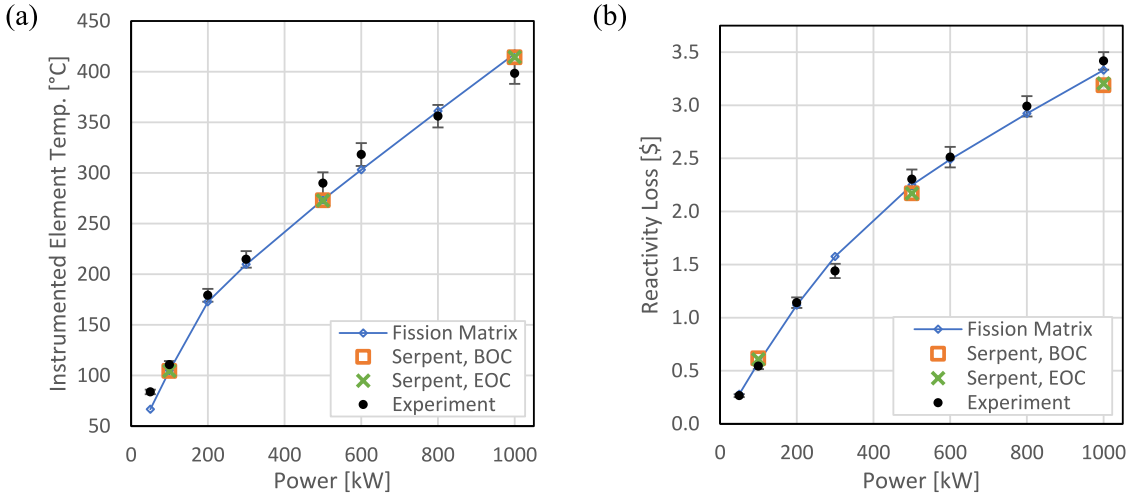

Fig. 13. Comparison of (a) instrumented element temperature and (b) reactivity loss calculated using different neutronics methods and core burnup.

Table 2
Differences in multiplication factor and 3D fission source between case with TRACE-FM fuel temperature distribution and case with uniform fuel temperature. Cases at a given power level have the same average temperature.

Power [kW]	Multiplication Factor			3D Fission Source	
	Calculated T. Distribution [-]	Uniform T. Distribution [-]	Rel. Difference [pcm]	RMS Rel. Difference [%]	Max. Rel. Difference [%]
50	1.000003	1.000478	47.5	0.2	−0.5
100	1.000003	1.000861	85.9	0.3	−0.8
200	0.999999	1.001573	157.3	0.5	1.3
300	1.000003	1.002036	203.3	0.6	−1.7
500	0.999996	1.002109	211.2	0.7	−2.1
600	0.999997	1.002183	218.6	0.7	−2.2
800	1.000005	1.002571	256.6	0.9	−2.7
1000	1.000001	1.003052	305.1	1.1	−3.1

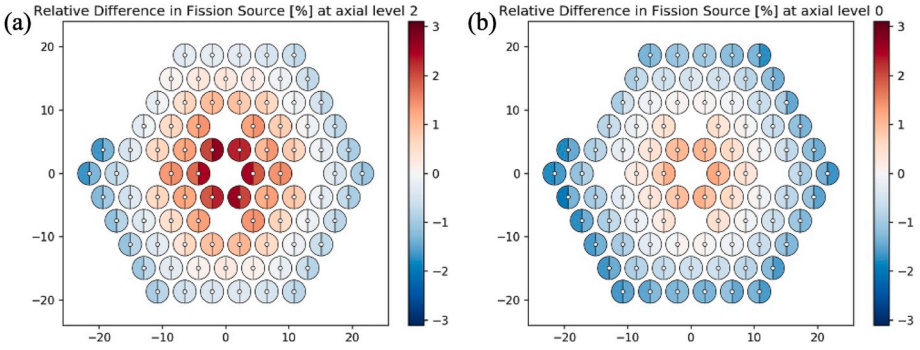

Fig. 14. Relative difference between fission sources from non-uniform and uniform fuel temperature cases at 1000 kW nominal power (a) in the axial center of the core and (b) at the bottom of the core.

Table 3
Differences in multiplication factor and 3D fission source between TRACE-FM iteration with a fuel temperature distribution and TRACE-FM iteration with uniform fuel temperature.

Power [kW]	Multiplication Factor			3D Fission Source	
	Calculated T. Distribution [-]	Uniform T. Distribution [-]	Rel. Difference [pcm]	RMS Rel. Difference [%]	Max. Rel. Difference [%]
50	1.000003	0.999998	−0.5	0.3	−1.3
100	1.000003	0.999997	−0.6	0.6	−3.1
200	0.999999	1.000000	0.1	1.3	−8.1
300	1.000003	1.000002	−0.1	2.4	−13.3
500	0.999996	0.999995	−0.2	2.7	−14.7
600	0.999997	0.999997	0.0	2.3	−13.1
800	1.000005	1.000002	−0.3	2.0	−11.9
1000	1.000001	0.999995	−0.6	1.9	−10.1

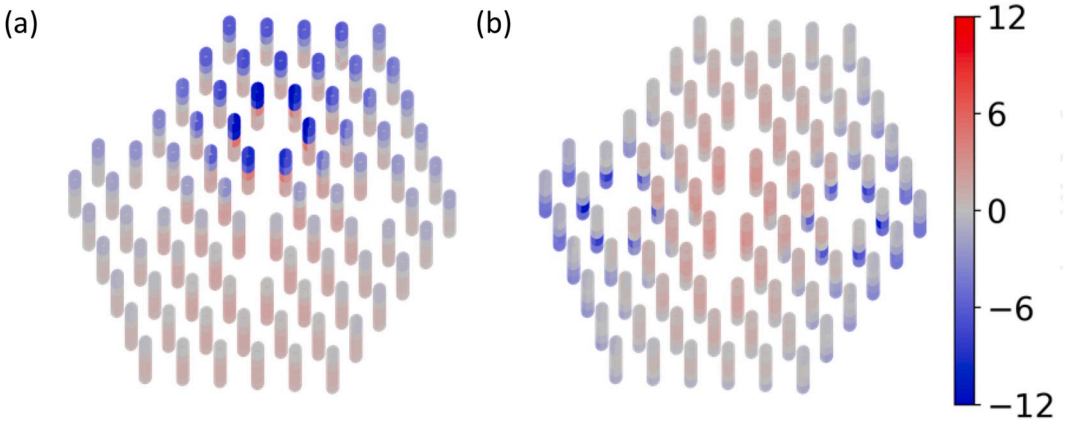

Fig. 15. Relative differences between steady-state power profiles for TRACE-FM iteration with temperature distributions and TRACE-FM iteration with uniform temperature, for (a) 300 kW and (b) 1000 kW.

movement, which also affects the power shape. An iterative TRACE-FM simulation with uniform fuel temperature profiles was run and compared to the case with temperature distributions. Results of this are shown in Table 3.

As expected, the difference between multiplication factors is minimal, since in both cases the control rods are adjusted to critical. RMS and maximum fission source are larger, and are generally greater when the reactivity difference discussed in Table 2 is greater. Differences also peak at 500 kW; this is because the rods are near the core periphery, so more physical rod movement is needed to compensate for the difference in reactivity. This has a greater impact on local power. This can be seen for the 300 kW case in Fig. 15, where the safety rod is almost fully withdrawn so the local power near the top of the core is affected. In contrast, rod movement is near the center of the core in the 1000 kW case, so local differences are smaller.

As Fig. 15 shows, control rod position can also have a significant impact on the power shape. Different control rod operation schemes were discussed in Section 3.3; the sensitivity of the power shape to these different schemes is shown in Table 4. Largest differences tend to occur around the 300 kW power level, when the "simulate operation" scheme has the shim and regulating rods fully inserted, but the safety and transient rod are almost fully withdrawn. Differences are plotted in Fig. 16. Differences are calculated as

$$Diff = \left(p_{rodEven} - p_{simOp}\right) / \left(p_{simOp}\right) \times 100$$

Despite large differences observed at specific locations, the choice of rod operation scheme has little impact on the instrumented section of fuel, which explains why the validation is relatively insensitive to this parameter. Due to the large differences observed in the power profiles used for different rod operation schemes, it is recommended to include this data, if possible, in a future depletion calculation scheme. Future work will investigate integrating xenon depletion into the present calculation scheme and examining these effects on depletion of the core.

5. Summary and conclusion

A coupled neutronics/thermal hydraulics model was developed for the PSBR initial core loadings. In the coupled model, TRACE was used for thermal hydraulics, and a fission matrix interpolation method using a Serpent-generated database was used for neutronics. For the TRACE-FM model, best estimates for instrumented element temperature match experimental data with an RMS relative difference of 8.3% and a max relative difference of −20.5%. It is worth noting that the largest difference occurs only in the lowest power level, and agreement for other points is generally good. Reactivity loss from thermal-hydraulic effects matches experiment data with an RMS difference of 4.5% and a maximum difference of 9.5%. Validation is somewhat limited because only one instrumented element was loaded in the oldest fresh core loadings. Next, these results should be used to perform depletion calculations for the PSBR. Once depletion calculations have been performed, further validation can be carried out on core loading patterns with more extensive data (e.g. experiments with instrumented elements placed in multiple locations).

Several areas of sensitivity were identified in the thermal-hydraulics model. Two of the most impactful parameters for validation on instrumented element temperature were the radial location of the thermocouple and the fuel-cladding gap heat transfer coefficient. Both of these parameters were estimated using data found in the PSBR safety analysis report for the reactor and from dimensional drawings originally furnished by the fuel's manufacturer.

Finally, the impact of some of the new phenomena explored by this model are examined. Modeling the fuel temperature profile instead of an average uniform fuel temperature was found to alter the 3D fission source distribution by up to 5%, or up to 20% if errors in multiplication factor estimation were allowed to propagate to control rod movement.

Table 4
Differences in 3D fission source between the "simulate operation" control rod operation scheme and the "rods even" operation scheme.

Power [kW]	RMS Rel. Difference [%]	Max. Rel. Difference [%]
50	19.1	86.6
100	19.5	87.4
200	20.6	89.5
300	22.1	92.3
500	19.0	85.4
600	17.7	68.8
800	15.9	62.5
1000	14.5	64.2

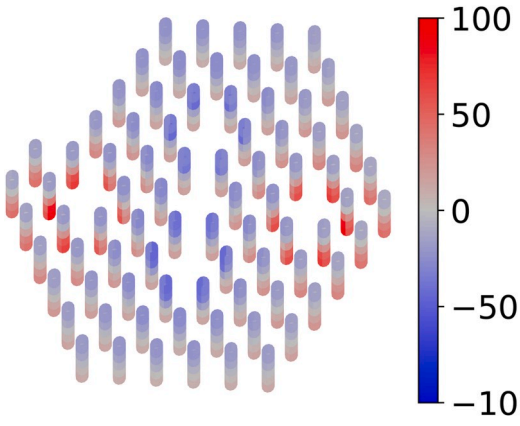

Fig. 16. Relative differences between power profiles using different rod operation schemes at 300 kW nominal power.

In general, control rod operation strategy was shown to have a large impact on the fission source profile, with local differences up to 92.3% being observed. The code developed in the present work has the capability to model these changes and in so doing improve the fidelity of the core management model used at the PSBR. One of the challenges in implementing this will be obtaining granular operation data so that the fidelity of the modeling approaches used can be fully exploited. Development of transient capabilities of the code and incorporation of xenon effects may also be important to realizing this objective.

Credit author statement

Adam Rau: Methodology, Software, Formal analysis, Investigation, Writing – Original Draft, Visualization, **William Walters:** Conceptualization, Methodology, Resources, Writing – Review & Editing, Supervision, Project Administration.

Declaration of competing interest

None.

Acknowledgment

This work was supported by the Nuclear Regulatory Commission Graduate Fellowship Program.

References

Alloni, D., et al., 2014. Final characterization of the first critical configuration for the TRIGA Mark II reactor of the University of Pavia using the Monte Carlo code MCNP. Prog. Nucl. Energy 74, 129. https://doi.org/10.1016/j.pnucene.2014.02.022. Elsevier Ltd.

Borio di Tigliole, A., et al., 2010. Benchmark evaluation of reactor critical parameters and neutron fluxes distributions at zero power for the TRIGA Mark II reactor of the

University of Pavia using the Monte Carlo code MCNP. Prog. Nucl. Energy **52** 5, 494. https://doi.org/10.1016/j.pnucene.2009.11.002. Elsevier Ltd.
Boyle, P.G., Hughes, D.E., Levine, S.H., 1998. A new fuel management plan for the Pennsylvania state university TRIGA reactor including supporting experiments and calculations. Nucl. Technol. **123** 2, 222. https://doi.org/10.13182/nt98-a2894.
Cammi, A., et al., 2016. Characterization of the TRIGA Mark II reactor full-power steady state. Nucl. Eng. Des. 300, 308. https://doi.org/10.1016/j.nucengdes.2016.01.026. Elsevier B.V.
Carney, S., et al., 2014. Theory and applications of the fission matrix method for continuous-energy Monte Carlo. Ann. Nucl. Energy 73, 423. https://doi.org/10.1016/j.anucene.2014.07.020. Elsevier Ltd.
Dufek, J., Gudowski, W., 2009a. Fission matrix based Monte Carlo criticality calculations. Ann. Nucl. Energy **36** 8, 1270. https://doi.org/10.1016/j.anucene.2009.05.003. Elsevier Ltd.
Dufek, J., Gudowski, W., 2009b. Stability and convergence problems of the Monte Carlo fission matrix acceleration methods. Ann. Nucl. Energy **36** 10, 1648. https://doi.org/10.1016/j.anucene.2009.07.020. Elsevier Ltd.
Dufek, J., Holst, G., 2016. Correlation of errors in the Monte Carlo fission source and the fission matrix fundamental-mode eigenvector. Ann. Nucl. Energy 94, 415. https://doi.org/10.1016/j.anucene.2016.04.013. Elsevier Ltd.
Garfola, S., et al., 2014. Thermal-hydraulic Design Analysis of the Penn State Breazeale Nuclear Rector. State College, PA.
Gougar, H.D., 1997. Development and Modeling of Coolant Flow Control in the Penn State Breazeale Reactor. Penn State University.
Haag, J.A., Levine, S.H., 1973. Thermal analysis of the Pennsylvania state university Breazeale nuclear reactor. Nucl. Technol. **19** 1, 6. https://doi.org/10.13182/nt73-a31313.
Harris, B.K., Walters, W.J., 2019. Evaluation of updated Monte Carlo models for the Penn state Breazeale reactor. Trans. Am. Nucl. Soc. 121, 1529–1531. Washington, DC.
He, D., Walters, W.J., 2019. A local fission matrix correction method for heterogeneous whole core transport with RAPID. Ann. Nucl. Energy 134, 263. https://doi.org/10.1016/j.anucene.2019.06.008. Elsevier Ltd.
Henry, R., Tiselj, I., Snoj, L., 2017. CFD/Monte-Carlo neutron transport coupling scheme, application to TRIGA reactor. Ann. Nucl. Energy 110, 36. https://doi.org/10.1016/j.anucene.2017.06.018. Elsevier Ltd.
Henry, R., Tiselj, I., Snoj, L., 2018. Transient CFD/Monte-Carlo Neutron Transport Coupling Scheme for simulation of a control rod extraction in TRIGA reactor. Nucl. Eng. Des. **331** (March), 302. https://doi.org/10.1016/j.nucengdes.2018.03.015. Elsevier.
Karriem, V.V., 2016. The Development of a Thermal Hydraulic Feedback Mechanism with a Quasi-Fixed Point Iteration Scheme for Control Rod Position Modeling for the TRIGSIMS-TH Application. Penn State University.
Kitada, T., Takeda, T., 2001. Effective convergence of fission source distribution in Monte Carlo simulation. J. Nucl. Sci. Technol. 38 5, 324. https://doi.org/10.1080/18811248.2001.9715036.
Laureau, A., et al., 2015. Transient Fission Matrix: kinetic calculation and kinetic parameters beta effective and Lambda effective. Ann. Nucl. Energy 85, 1035. https://doi.org/10.1016/j.anucene.2015.07.023. Elsevier Ltd.
Laureau, A., et al., 2017. Transient coupled calculations of the molten salt fast reactor using the transient fission matrix approach. Nucl. Eng. Des. 316, 112. https://doi.org/10.1016/j.nucengdes.2017.02.022. Elsevier B.V.
Leppänen, J., et al., 2015. The Serpent Monte Carlo code: status, development and applications in 2013. Ann. Nucl. Energy 82, 142. https://doi.org/10.1016/j.anucene.2014.08.024.
Mesquita, A.Z., 2006. Experimental heat transfer analysis of the IPR-R1 TRIGA reactor. In: International Conference on Research Reactors, Sydney, Australia.
Naughton, W.F., et al., 1974. Triga core management model. Nucl. Technol. **23** 3, 256. https://doi.org/10.13182/nt74-a15918.
Radiation Science And Engineering Center, 2005. Safety Analysis Report for the Renewal of License R-2 for the Breazeale Nuclear Reactor. State College, PA.
Rau, A., Walters, W.J., 2019a. Fission matrix neutronics calculations with temperature feedback in a nuclear thermal propulsion core. In: Nuclear and Emerging Technologies for Space, American Nuclear Society Topical Meeting Richland, WA, February 25 – February 28, 2019. American Nuclear Society, Richland, WA.
Rau, A., Walters, W.J., 2019b. Fission matrix methods for nuclear thermal propulsion applications. In: International Conference on Mathematics and Computational Methods. American Nuclear Society, Portland, Oregon.
Ross, D.A., 1969. The Pennsylvania State University TRIGA Reactor Description, Initial Testing, and First Three Years of Operation. Penn State University.
Şahin, D., Ünlü, K., 2012. Determination of self shielding factors and gamma attenuation effects for tree ring samples. J. Radioanal. Nucl. Chem. 291 2, 549. https://doi.org/10.1007/s10967-011-1281-x.
Simnad, M.T., 1981. The UZrHx alloy: its properties and use in TRIGA fuel. Nucl. Eng. Des. **64** 3, 403. https://doi.org/10.1016/0029-5493(81)90135-7.
Terlizzi, S., Kotlyar, D., 2019. Fission matrix decomposition method for criticality calculations: theory and proof of concept. Nucl. Sci. Eng. 1. https://doi.org/10.1080/00295639.2019.1583948. Taylor & Francis.
Tippayakul, C., Ivanov, K., Frederick Sears, C., 2008. Development of a practical Monte Carlo based fuel management system for the Penn state university Breazeale research reactor (PSBR). Ann. Nucl. Energy **35** 3, 539. https://doi.org/10.1016/j.anucene.2007.07.013.
Tippayakul, C., et al., 2004. Automated three dimensional depletion capability for the Pennsylvania State University research reactor. In: PHYSOR 2004 - the Physics of Fuel Cycles and Advanced Nuclear Systems 51 January. Lagrange Park, IL.
Topham, T.J., Rau, A., Walters, W.J., 2020. An iterative fission matrix scheme for calculating steady-state power and critical control rod position in a TRIGA reactor. Ann. Nucl. Energy. 135 https://doi.org/10.1016/j.anucene.2019.106984.
Topham, T.J., Walters, W.J., 2018. Temperature feedback using the fission matrix for a TRIGA reactor. Trans. Am. Nucl. Soc. 119 (July), 1233.
Tuominen, R., Valtavirta, V., Leppänen, J., 2019. New energy deposition treatment in the Serpent 2 Monte Carlo transport code. Ann. Nucl. Energy 129, 224. https://doi.org/10.1016/j.anucene.2019.02.003. Elsevier Ltd.
Uçar, D., Ünlü, K., Heidrich, B.J., 2014. Thermal-Hydraulics Analysis Of A New Core-Moderator Assembly Design For The Penn State Breazeale Reactor Using Ansys Fluent Code.
U.S.NRC, 2017. TRACE V5.0 Patch 5 Theory Manual – Field Equations, Solution Methods, and Physical Models.
Walters, W.J., Roskoff, N.J., Haghighat, A., 2018. The RAPID fission matrix approach to reactor core criticality calculations. Nucl. Sci. Eng. 192 1, 21. https://doi.org/10.1080/00295639.2018.1497395. Taylor & Francis.
Walters, W., et al., 2009. Calculation of sub-critical multiplication using a simplified fission matrix method. Trans. Am. Nucl. Soc. 101 1, 447.
Wargon, M., 2015. Safety Analysis of the New Core-Moderator Assembly for the Penn State Breazeale Nuclear Reactor. Penn State University.
X-5 Monte Carlo Team, 2008. MCNP - A General Monte Carlo N-Particle Transport Code.
IAEA, 1992. Research Reactor Core Conversion Guidebook Volume 4: Fuels. Vienna, Austria.